A New Look at the Primary Charge Separation in Bacterial Photosynthesis†

Spiros S. Skourtis,‡ Antonio J. R. da Silva,§ William Bialek,⊥ and José N. Onuchic*,‡

Department of Physics, University of California, San Diego, La Jolla, California 92093; Department of Physics, University of California, Berkeley, Berkeley, California 94720; and N.E.C. Research Institute, 4 Independence Way, Princeton, New Jersey 08540 *(Received: February 11, 1992; In Final Form: June 18, 1992)*

A theory for the primary charge separation in photosynthetic bacteria is presented. We propose that this reaction may lie in a regime that is different from the traditional nonadiabatic (golden rule) regime. In the context of the primary charge separation, the assumption of nonadiabaticity implies that vibrational relaxation in $(BChl)_2^+(BPh)^-$ is much faster than the electron-transfer rate from $(BChl)_2^*$ to BPh (i.e., much faster than a picosecond). Instead, we propose that vibrational relaxation in the charge-separated state might well compete with the rate of initial electron transfer. To describe such a regime, we abandon the nonadiabatic theory and suggest that in the case of this reaction, the vibronic mixings between initial and final vibronic states are of the same order of magnitude as the vibronic widths of the final states. When this is true, the transfer rate competes with relaxation in the final vibronic manifold. We show that the proposed regime is plausible for the primary charge separation since it predicts reasonable values for the relevant parameters of the reacting system (vibronic mixings, widths, etc.), and it is consistent with several recent experiments. It also explains the robustness of the primary rate to changes in the energy gap, temperature, and initial excitation in P*I.

Introduction

Bacterial photosynthesis has attracted the attention of theorists and experimentalists for more than two decades.[1] Although great progress has been made toward a better understanding of the mechanisms involved,[2-4] there remain important questions without conclusive answers.[5,6] The best example is the primary charge separation from the bacteriochlorophyll dimer to the bacteriopheophytin ($P^*I \rightarrow P^+I^-$). This reaction has been the subject of extensive theoretical and experimental work[5,6] because it involves an exceptionally fast electronic transfer (3 ps), over a large distance (17 Å center-to-center).[6] This remarkable speed greatly contributes to the high efficiency (close to unity) of the overall charge separation ($P^*Q_B \rightarrow P^+Q_B^-$) in the reaction center. Two mechanisms have been proposed to explain this rate. In one, the bacteriochlorophyll monomer which lies between the dimer and the bacteriopheophytin acts as a virtual intermediate for the transferring electron.[7-9] In the other it acts as a real intermediate.[10,11] It has also been suggested that the two mechanisms work in parallel.[12,13] There are still no experimental data which clearly distinguish between these possibilities.[14-17] All mechanisms adopt a perturbative treatment for the primary transfer. The rate is given by the nonadiabatic (golden rule) expression

$$\text{rate} = (2\pi V_{el}^2/\hbar)F \qquad (1)$$

where V_{el} is the mixing between initial and final (or intermediate) electronic states, and F is a Franck–Condon averaged density of vibrational states.

The golden rule approximation is based on the assumption that the mixings between initial and final vibronic states are much smaller than the widths of the final vibronic states.[18] In this case the rate is much slower than the vibrational relaxation rate of the final states. We argue that the golden rule regime may not be appropriate for the primary charge separation. This reaction involves an ultrafast electron transfer (3 ps) which could actually compete with vibrational relaxation in the final vibronic manifold.

Instead, we propose that the primary charge separation may lie in a different regime where the mixings between initial and final states are of the same order of magnitude as the widths of the final states. In this regime it is shown that the rate competes with relaxation in the final vibronic manifold ($\tau_{rate} \sim \tau_{rel}$), as may well be the case for the primary transfer. We are then able to explain the fast primary rate for reasonable values of the parameters of the reacting system (energy gap, vibronic mixings, vibronic widths, and vibrational frequencies). Equally important, the rate in this regime is shown to be robust to changes in all of these parameters. This robustness is better than that exhibited by golden rule theories and can explain several temperature, energy gap, and hole-burning experiments which suggest that the dependence of the primary rate on the degree of initial excitation in P*I is slow (only 20% change in the rate when the degree of initial excitation in P*I varies by a few hundred wavenumbers).

Shortly after we obtained these results,[19] we received the paper by Vos et al.[20] which demonstrates that the regime we have identified is indeed of relevance to the primary charge separation. We discuss in detail the way in which their experiment provides evidence in favor of our predictions. We also correlate their results with the temperature and energy gap experiments mentioned above, and we reinterpret several other experiments in terms of this regime.

Definition of the Rate

In our analysis of the primary charge separation, we use the model shown in Figure 1 where a manifold $\{|i\rangle_{P^*I}\}$ of initial vibronic states of P*I is coupled to a manifold $\{|n\rangle_{P^+I^-}\}$ of final vibronic states of P^+I^-. A vibronic state is a combination of an electronic and a nuclear-vibrational state. The vibronic couplings between initial and final states are denoted by $\Delta_{i,n}$ and each state $|n\rangle_{P^+I^-}$ is assigned a width $\hbar\Gamma$.[21] According to the Franck–Condon approximation, the electronic transfer corresponds to a vertical "flip" between the energy surfaces $E_{P^*I}(R)$ and $E_{P^+I^-}(R)$, at some nuclear position R_0. Energy conservation requires that R_0 is the crossing point of the two energy surfaces. The vibronic couplings $\Delta_{i,n}$ which induce the transfer at R_0 are then given by $\Delta_{i,n} = V_{el}(R_0)(FC_{in})^{1/2}$. $V_{el}(R_0)$ is the electronic matrix element between P*I and P^+I^-, evaluated at R_0. FC_{in} is the Franck–Condon factor between the vibrational components of $|i\rangle_{P^*I}$ and $|n\rangle_{P^+I^-}$. The model of Figure 1 and several of its variations are often used to study radiationless transitions[22-24] such as the primary charge separation.

The fundamental quantity of interest to the study of the primary rate is the inverse lifetime of $|i\rangle_{P^*I}$ which corresponds to the average rate of decay of the vibronic state. It is given by

$$\tau_i^{-1} = \int_0^\infty dt\, P_i(t) \Big/ \int_0^\infty dt\, tP_i(t) \qquad (2)$$

† This work was completed in part when the first author was a graduate student at the Department of Biophysics, University of California, Berkeley.
‡ University of California, San Diego.
§ University of California, Berkeley.
⊥ N.E.C. Research Institute.
* To whom correspondence should be addressed.

0022-3654/92/2096-8034$03.00/0

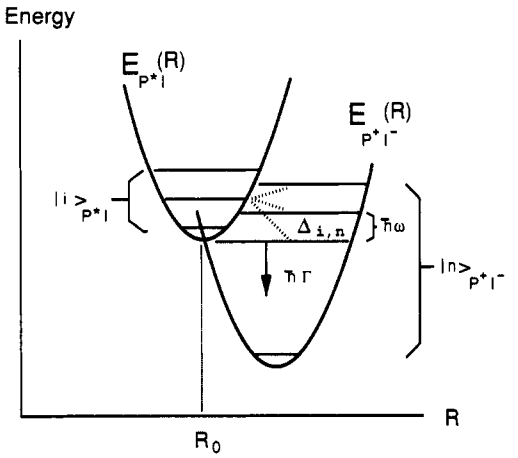

Figure 1. Model used to describe the primary electron transfer. The reaction can be thought of as the decay of an initial manifold of vibronic states of P*I $\{|i\rangle_{P^*I}\}$, into a final manifold of vibronic states of P^+I^- $\{|n\rangle_{P^+I^-}\}$. The decay is caused by the vibronic coupling between initial and final states $\Delta_{i,n} = V_{el}(FC_{i,n})^{1/2}$.

where $P_i(t) = |\langle i|e^{-i\hat{H}t/\hbar}|i\rangle|^2$ is the survival probability for state $|i\rangle_{P^*I}$. The corresponding decay amplitude is

$$\langle i|e^{-i\hat{H}t/\hbar}|i\rangle = \frac{1}{2\pi i}\int_C d\tilde{E}\, e^{-i\tilde{E}t/\hbar}\langle i|G(\tilde{E})|i\rangle \tag{3}$$

where (Appendix I)

$$\langle i|G(\tilde{E})|i\rangle = \frac{1}{\tilde{E} - E_i - V_{el}^2\sum_n (FC_{i,n})\dfrac{(\tilde{E} - n\hbar\omega - i\hbar\Gamma/2)}{(\tilde{E} - n\hbar\omega)^2 + (\hbar\Gamma/2)^2}} \tag{4}$$

The calculation of the decay amplitude (eq 3) amounts to finding the residues of the Green's function (eq 4)[25] at its different poles $\tilde{E}_m$ and then using the residue theorem.

Golden Rule Approximation and Its Implications to the Primary Charge Separation

The golden rule expression for the rate (eq 1) is obtained by letting the vibronic mixings be much less than the vibronic widths ($V_{el}(FC_{i,n})^{1/2} \ll \hbar\Gamma$ in eq 4).[26] In this limit only one pole survives and the decay amplitude (eq 3) is pure exponential (Appendix I). The golden rule rate is then given by

$$\tau_i^{-1} = 2\pi V^2 F/\hbar \tag{5}$$

where

$$F = \sum_n (FC_{i,n})\frac{1}{\pi}\frac{\hbar\Gamma/2}{(E_i - n\hbar\omega)^2 + (\hbar\Gamma/2)^2} \tag{6}$$

F, the density of states seen by $|i\rangle_{P^*I}$, gives the energy gap dependence of the primary rate. It is a Franck–Condon-weighted sum of Lorentzians of width $\hbar\Gamma$, separated by $\hbar\omega$.[27]

To get the relative magnitudes of the parameters involved in this approximation, we rewrite the rate (eqs 5 and 6) in dimensionless form:

$$\frac{\tau_i^{-1}}{\Gamma} = 2\pi(V_{el}/\hbar\Gamma)^2\sum_n (FC_{i,n})\frac{1}{\pi}\frac{1/2}{((E_i - n\hbar\omega)/\hbar\Gamma)^2 + (1/2)^2} \tag{7}$$

For the above expression to be valid the vibronic mixings must be much less than the vibronic widths ($V_{el}(FC_{i,n})^{1/2}/\hbar\Gamma \ll 1$). If $\hbar\omega$ and $\hbar\Gamma$ are reasonable, so that the Lorentzian sum remains finite, then the following relation holds: $\tau_i^{-1}/\Gamma \propto FC_{i,n}(V_{el}/\hbar\Gamma)^2 \ll (FC_{i,n})^{1/2}V_{el}/\hbar\Gamma$. We conclude that in the golden rule regime certain energy scales associated with the reaction are widely separated:[28]

$$\hbar(\tau_i^{-1}) \ll (FC_{i,n})^{1/2}V_{el} \ll \hbar\Gamma \le \hbar\omega \tag{8}$$

Golden Rule Approximation in Terms of Time Scales. We now define two important time scales relevant to this discussion,[29-31]

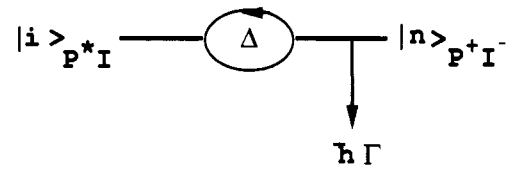

Figure 2. Simple model for the decay of an initial vibronic level of P*I into a final resonant vibronic level of P^+I^-.

the vibronic mixing time τ_{mix} (or equivalently the electronic mixing time τ_{mix}^{el}), and the vibronic relaxation time τ_{rel}. The vibronic mixing time is a measure of the time it takes for an initial vibronic level $|i\rangle_{P^*I}$ to mix into a final level $|n\rangle_{P^+I^-}$ (Figure 2). It is given by $\tau_{mix} = \hbar/\Delta_{i,n}$ (the electronic mixing time is given by $\tau_{mix}^{el} = \hbar/V_{el}$). The vibronic relaxation time is just the lifetime of the final levels $\{|n\rangle_{P^+I^-}\}$ given by $\tau_{rel} = 1/\Gamma$. In terms of these time scales, eq 8 becomes

$$2\pi\tau_i \gg \tau_{mix} = \tau_{mix}^{el}/(FC_{in})^{1/2} \gg 2\pi\tau_{rel} \ge \tau_{per} \tag{9}$$

where $\tau_{per} = 2\pi/\omega$ is the characteristic period of oscillation of the nuclear reaction coodinate. In the golden rule regime, the lifetime of the initial vibronic state is much greater than the mixing time between initial and final states, which in turn is much greater than the relaxation time of the final states. In other words, for a golden rule theory to be valid, there must be a large separation of certain time scales. This result (eq 9) should be kept in mind to better understand the arguments we will be presenting in the next section.

If we substitute for the low temperature primary rate ($\tau_i \sim$ ps) in eq 9, we get $\tau_{rel} \ll 1$ ps. Therefore, if the primary charge separation were to lie in the golden rule regime, the vibrational relaxation time in P^+I^- would be much less than a picosecond. There are currently no experiments which measure τ_{rel} in P^+I^-. However, vibrational lifetimes of optical phonons in solids are of the order of a picosecond.[32,33] Lifetimes of picoseconds have also been observed in activated processes in proteins,[34] using molecular dynamics simulations. It is therefore possible that golden rule overestimates the rate of vibrational relaxation in P^+I^-. It might also underestimate the magnitude of the electronic mixing time (or equivalently overestimate the electronic matrix element).

Nonperturbative Theory

In the discussion which follows we will often identify the initial vibronic state $|i\rangle_{P^*I}$ in Figure 1 with the ground vibronic state $|0\rangle_{P^*I}$. We are allowed to do this since the primary rate is of the same order of magnitude for both low and room temperatures (see discussion of experiments). Also, as it will become apparent later, the arguments presented here do not depend on the particular choice for initial vibronic state of P*I. This choice just makes the discussion more tractable.

Motivation. Consider the average decay rate of $|i\rangle_{P^*I}$ resonantly coupled to only one final state $|n\rangle_{P^+I^-}$, shown in Figure 2. Expressed in units of Γ the decay rate is (Appendix II)

$$\frac{\tau_i^{-1}}{\Gamma} = \frac{4^4x^6 + 3.4^2x^4 - 4x^2}{2.4^4x^6 - 2.4^2x^4 + 4^2x^2 - 1} \tag{10}$$

where $x = \Delta/\hbar\Gamma$. A plot of τ_i^{-1}/Γ as a function of x is shown in Figure 3. This plot allows us to identify the different regimes of the rate as a function of Δ in units of Γ. We see that for $0.5 \le x \le 1$, the rate is close to its optimal value Γ ($0.6 \le \tau_i^{-1}/\Gamma \le 0.7$). The variation of the rate with respect to Δ is slow in this region (linear with slope 1 for $0.4 < x < 0.6$ and with slope -0.2 for $0.6 < x < 1$). We call this region optimal. For $x \le 0.1$ ($\Delta \le 0.1\hbar\Gamma$) the rate shows a quadratic dependence with respect to Δ, and this region describes the regime where golden rule is exact, given by eq 8. For $x \ge 1$ ($\Delta \ge \hbar\Gamma$) the rate approaches the value of 0.5Γ and its variation with respect to Δ is extremely slow. This is the overcoupled regime. The existence of the optimal regime implies that

$$\text{if } \Delta_{i,n} \sim \hbar\Gamma \quad \text{then } \hbar\tau_i^{-1} \sim \Delta_{i,n} \sim \hbar\Gamma \tag{11}$$

In this regime the vibronic coupling is similar to the vibronic width, and the decay rate (in units of energy) is approximately equal

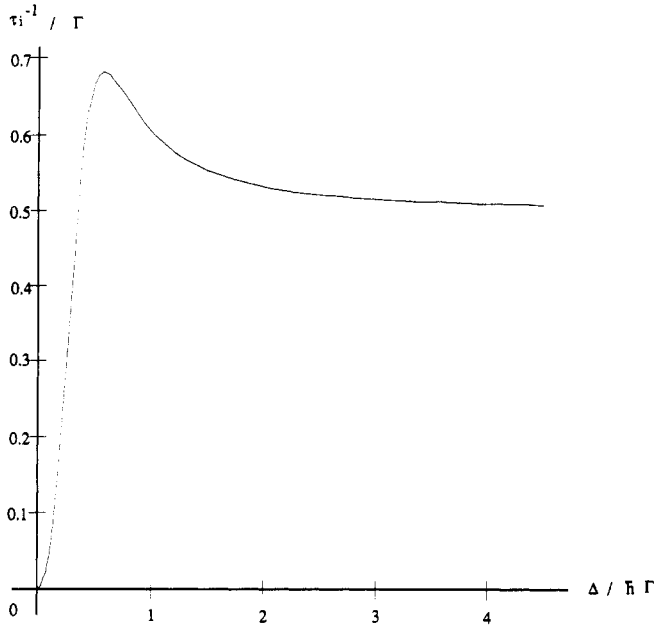

Figure 3. Plot of the decay rate of $|i\rangle_{P^*I}$ as a function of the vibronic coupling Δ, in units of the vibronic width of the final state Γ. The configuration is that given by Figure 2.

to these two parameters. In the language of the time scales defined earlier, the mixing time is similar to the relaxation time, and the lifetime of the initial state is of the same order of magnitude as these two times:

$$\begin{aligned} &\text{if} \quad \tau_{mix} = \tau_{el}^{mix}/(FC_{in})^{1/2} \sim 2\pi\tau_{rel} \\ &\text{then} \quad 2\pi\tau_i \sim \tau_{mix} \sim 2\pi\tau_{rel} \end{aligned} \tag{12}$$

We emphasize that the regime defined by eqs 11 and 12 is optimal; the electron-transfer rate approaches the rate of vibrational relaxation of the final vibronic state. Also, the rate in this regime requires a much smaller matrix element than the corresponding golden rule rate to achieve the same speed (i.e., $\hbar(\tau_i^{-1}) \sim V_{el}(FC)^{1/2}$ as opposed to the golden rule case where $\hbar(\tau_i^{-1}) \ll V_{el}(FC)^{1/2}$.[35] The question to be answered is whether or not the primary charge separation lies in the optimal regime.

To address this question, we let τ_i in eq 12 equal the low-temperature primary rate (~1 ps). We then find that the vibronic mixing time and the vibronic relaxation time must be of the order of 6 and 1 ps, respectively ($2\pi\tau_i \sim 6$ ps $\sim \tau_{mix}^{el}/(FC_{in})^{1/2} \sim 2\pi\tau_{rel}$). As already argued in our discussion of the golden rule approximation, although there are no experiments that directly measure vibronic relaxation in P^+I^-, relaxation times of the order of a picosecond are reasonable. Furthermore, if we choose $(FC_{in})^{1/2} = 0.2$ (a value consistent with experiments[36]), we predict a magnitude for τ_{mix}^{el} corresponding to $V_{el} \sim 30$ cm^{-1} which is also plausible.[37] Another piece of supporting evidence comes from several energy gap, temperature, and hole-burning experiments,[38-43] which suggest that the primary rate is not considerably affected by changes in the vibronic excitation of P*I. This robustness is a consequence of the fact that in the optimal regime (eqs 11 and 12), the rate shows a slow variation (at most linear) with respect to the vibronic mixing. So the rate changes slowly with respect to changes in the electronic matrix element or the Franck–Condon factor. On the other hand in the golden rule regime the dependence on vibronic coupling is stronger since it is quadratic. We give a detailed discussion of all the relevant experiments later.

A problem with the simple model of Figure 2 is the assumption of resonance between initial and final states. Surely, one cannot expect that a vibronic state of P*I always finds a resonant vibronic state of P^+I^- to couple to. However, it can find nearly resonant states if the $\{|n\rangle_{P^+I^-}\}$ spectrum is dense enough. The condition of near resonance is obtained if the energy spacing of the final states is of the same order of magnitude as their energy widths.

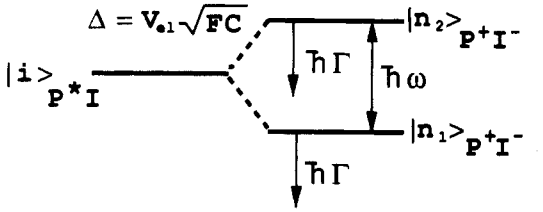

Figure 4. More realistic model for the decay of vibronic states of P*I into vibronic states of P^+I^-. The possibility of off resonance has been taken into account.

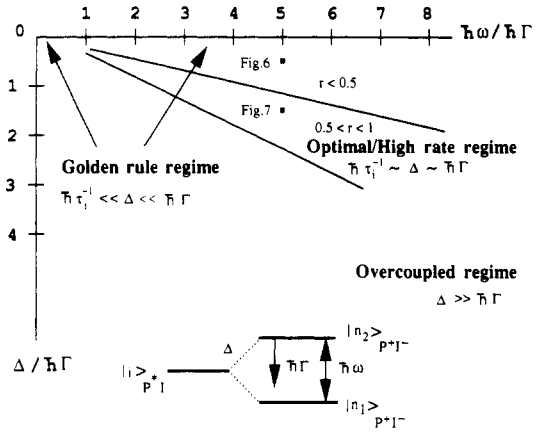

Figure 5. Plot of the different regimes of the decay rate of $|i\rangle_{P^*I}$ as a function of $\hbar\omega$ and Δ, in units of $\hbar\Gamma$. The configuration of Figure 4 is adopted.

Optimal Rate Regime. To quantitatively check this possibility and to introduce another relevant parameter to the problem (the period of nuclear oscillations), we consider the simplest possible situation that captures all the relevant physics (Figure 4). We let $|i\rangle_{P^*I}$ couple to only two final states $|n\rangle_{P^+I^-}$ and compute the exact value of its decay rate τ_i^{-1} without any further approximations. As before, we want to study the decay rate of $|i\rangle_{P^*I}$ in units of Γ and as a function of $\Delta/\hbar\Gamma$ and $\hbar\omega/\hbar\Gamma$. We are only interested in the rate when $|i\rangle_{P^*I}$ lies between $|n_1\rangle_{P^+I^-}$ and $|n_2\rangle_{P^+I^-}$. This is because within our approximation $|n_1\rangle_{P^+I^-}$ and $|n_2\rangle_{P^+I^-}$ represent the two final states which are closest in energy to $|i\rangle_{P^*I}$. For a fixed Γ, τ_i^{-1} is expected to reach a maximum when $|i\rangle_{P^*I}$ is close to $|n_1\rangle_{P^+I^-}$ or $|n_2\rangle_{P^+I^-}$, and a minimum when $|i\rangle_{P^*I}$ is halfway between $|n_1\rangle_{P^+I^-}$ and $|n_2\rangle_{P^+I^-}$. We study the ratio

$$r = (\tau_i^{-1})_{min}/(\tau_i^{-1})_{max} \tag{13}$$

as a function of these parameters. $(\tau_i^{-1})_{max}$ is just the maximum rate achieved when $|i\rangle_{P^*I}$ is close to $|n_1\rangle_{P^+I^-}$ or $|n_2\rangle_{P^+I^-}$. $(\tau_i^{-1})_{min}$ is the minimum rate reached when $|i\rangle_{P^*I}$ is halfway between the two final states. The rate is considered *optimal* if

$$0.5 \le r \le 1 \quad \text{and} \quad (\tau_i^{-1})_{max}/\Gamma \sim 1 \tag{14}$$

We then look for a whole range of values of $\Delta/\hbar\Gamma$ and $\hbar\omega/\hbar\Gamma$ which satisfy these two criteria. The constraint on r in eq 14 ensures that the decay rate is high enough even when the initial state is halfway between the two final states.

The results of these calculations are shown in Figure 5 together with the different regimes of the rate (Figures 6 and 7). As expected, the rate is optimal when the vibronic mixings and vibronic widths are of the same order of magnitude ($\hbar\Gamma \le \Delta \le 3\hbar\Gamma$). The vibronic energy spacings can be quite different ($\hbar\Gamma \le \hbar\omega \le 8\hbar\Gamma$). This regime is similar to the analogous regime of Figure 3 and is characterized by the relation[44]

$$\Delta_{i,n} \sim \hbar\Gamma \le \hbar\omega \tag{15}$$

from which it follows that

$$\hbar\tau_i^{-1} \sim (\Delta_{i,n}, \hbar\Gamma) \le \hbar\omega \tag{16}$$

In terms of time scales, we have shown that

$$\begin{aligned} &\text{if} \quad \tau_{mix} \sim 2\pi\tau_{rel} \ge \tau_{per} \\ &\text{then} \quad 2\pi\tau_i \sim \tau_{mix} \sim 2\pi\tau_{rel} \ge \tau_{per} \end{aligned} \tag{17}$$

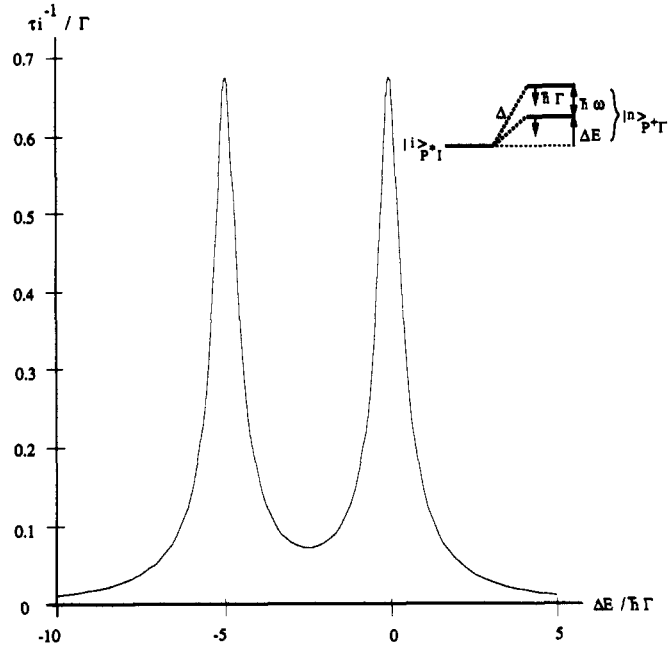

Figure 6. Behavior of the decay rate of $|i\rangle_{P^*I}$ as it moves from resonance to off resonance with respect to $|n\rangle_{P^+\Gamma^-}$. The values of $\Delta/\hbar\Gamma$ and $\hbar\omega/\hbar\Gamma$ are chosen in different rate regimes (see Figure 5). Here, $\Delta/\hbar\Gamma = 0.5$, $\hbar\omega/\hbar\Gamma = 5$.

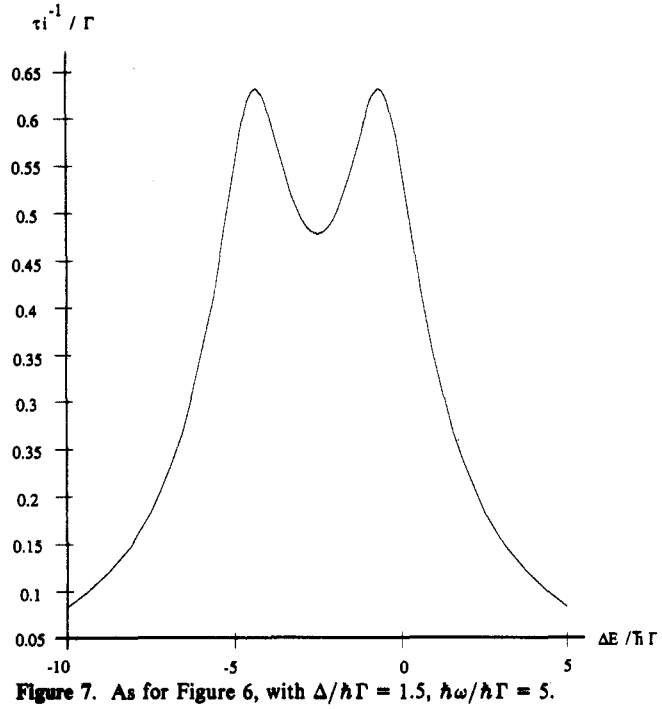

Figure 7. As for Figure 6, with $\Delta/\hbar\Gamma = 1.5$, $\hbar\omega/\hbar\Gamma = 5$.

When we substitute for the low-temperature primary rate in eqs 16 and 17 we get $\tau_{mix} \sim 2\pi\tau_{rel} \sim 6$ ps, as before, and $\tau_{per} \leq 6$ ps. The last prediction means that a low-frequency ($\tau_{per} \leq 6$ ps) possibly underdamped mode ($\tau_{rel} \sim$ ps), must couple to the primary transfer if the reaction is to lie in the optimal regime. This is consistent with the Vos experiment[20] which observes oscillations of 2 ps for a couple of periods in the dimer absorption and stimulated emission spectra. Furthermore, the simulations of Middendorf et al.[43] show that a low-frequency mode between 20 and 50 cm^{-1} might couple to the primary charge separation.

The calculations described here assume that a vibronic state of P*I couples to only two vibronic states of P^+I^-. This is not true in the regime we are studying since the vibronic mixings between initial and final vibronic levels are assumed to be similar to the widths and energy spacings of the final levels. However, coupling to additional final states does not alter the behavior of the rate

	$V_{el} \to \frac{1}{3} V_{el}$		$\hbar\Gamma \to \frac{1}{3}\hbar\Gamma$		$\hbar\omega \to 3\hbar\omega$	
Non pert. Start with: $\Delta/\hbar\Gamma = 1.5$ $\hbar\omega/\hbar\Gamma = 5$	$t_{max} = 1$	$t_{min} = 0.2$	$t_{max} = 0.9$	$t_{min} = 0.1$	$t_{max} = 0.9$	$t_{min} = 0.6$
Golden rule. Start with: $\Delta/\hbar\Gamma \ll 1$ $\hbar\omega/\hbar\Gamma = 5$	$t_{max} = 0.1$	$t_{min} = 0.1$	$t_{max} = 9$	$t_{min} = 0.25$	$t_{max} = 1$	$t_{min} = 0.25$

Figure 8. Illustration of the robustness of the decay rate of $|i\rangle_{P^*I}$ to changes in V_{el}, $\hbar\Gamma$, and $\hbar\omega$. t_{max} is the fractional change when there is resonance between initial and final states. t_{min} is the fractional change when $|i\rangle_{P^*I}$ is halfway inbetween $|n\rangle_{P^+\Gamma^-}$. The optimal and golden rule regimes are compared.

in this regime. When one adds more states above and below $|n_1\rangle_{P^+\Gamma^-}$ and $|n_2\rangle_{P^+\Gamma^-}$ in Figure 4, one finds that the region of optimal rate is very similar to that calculated for two final states.

Robustness of the Optimal Rate. We have already argued that in the optimal and overcoupled regimes the rate varies very slowly with respect to vibronic mixing (at most a linear variation). This behavior, shown in Figure 3, also holds in a situation where the initial state is completely off resonance with respect to the final states (i.e., halfway between the final states as in Figure 4). If in this situation we fix $\hbar\omega$ and $\hbar\Gamma$ somewhere in the region of optimality (see Figure 5) and plot the rate as a function of Δ in units of Γ, we get a plot very similar to that of Figure 3. That is for Δ of the order of or greater than $\hbar\Gamma$ the rate varies very slowly with respect to Δ (at most linearly), and for Δ much less than $\hbar\Gamma$ the variation is quadratic (golden rule regime). In addition, the rate in the optimal regime is robust to changes in $\hbar\omega$ and $\hbar\Gamma$. To illustrate this behavior, we give some indicative examples.

For both golden rule and nonperturbative theories we compute the changes in $(\tau_i^{-1})_{min}$ and $(\tau_i^{-1})_{max}$ (see eq 13) caused by a variation of either V_{el}, $\hbar\Gamma$, or $\hbar\omega$, with the others held fixed. For the case of the nonperturbative theory the initial values of these parameters are chosen to lie in the region of optimal rate ($\Delta/\hbar\Gamma = 1.5$, $\hbar\omega/\hbar\Gamma = 5$). For the golden rule theory, $\Delta/\hbar\Gamma \ll 1$ and we only need to set $\hbar\omega/\hbar\Gamma = 5$ in order to make a meaningful comparison with the nonperturbative theory. Since we have an analytic expression for the golden rule rate (eqs 5 and 6), it is not necessary to fix the initial value of $\Delta/\hbar\Gamma$.

In Figure 8 we show the effect of a typical change in V_{el}, $\hbar\Gamma$, or $\hbar\omega$ on $(\tau^{-1})_{min}$ and $(\tau^{-1})_{max}$. $t_{min} = (\tau_{min}^{-1})_{final}/(\tau_{min}^{-1})_{initial}$ and $t_{max} = (\tau_{max}^{-1})_{final}/(\tau_{max}^{-1})_{initial}$, where "initial" and "final" refer to the initial and final values of the parameters we have chosen to vary. We see that the optimal rate is much more robust to changes in V_{el} (or FC) and $\hbar\Gamma$ than the golden rule rate. It is also more robust to changes in $\hbar\omega$ but not as much. Another characteristic of the optimal regime, which follows from eqs 13 and 14, is that the rate does not drop with loss of resonance as much as it does in the golden rule regime.

Discussion of the Relevant Experiments

In a recent experiment Vos et al.[20] have observed oscillations in the dimer absorption and stimulated emission spectra of mutant *R. capsulatus* and wildtype *R. sphaeroides* reaction centers. The mutants lack Bph and are therefore unable to undergo primary charge separation. Oscillations of 0.5 and 2ps periods were recorded in both absorption and stimulated emission spectra of the mutants. For the wildtype ones a 0.7-ps oscillation was seen in the absorption and a 2-ps oscillation in the stimulated emission. The oscillations were damped after a couple of periods for both mutant and wildtype reaction centers. As pointed out by Vos et al.,[20] these oscillations may be due to the coherent excitation of more than one electronic state and/or vibrational dynamics in the PI and P*I surfaces. If the vibrational dynamics interpretation is adopted, several conclusions may be drawn from these results: (a) The experiment shows that a low-frequency (period of 2 ps), underdamped mode is coupled to the stimulated emission from P*I. This suggests that such a mode may be coupled to the primary charge separation. (b) If it is assumed that vibrational relaxation in P^+I^- is not much faster than in P*I, then the observed damping of 2–4 ps in the oscillations suggests that for P^+I^-, τ_{rel}

$\leq$ 2–4 ps. (c) The observation of oscillations itself indicates that there can be no thermalization in P*I prior to electronic transfer. We emphasize that these inferences are based on the assumption that the oscillatory kinetics arise from vibrational dynamics. How are these inferences relevant to our work?

Suppose that the primary charge separation lies in the regime where all the relevant time scales of the reaction are of the same order of magnitude (eq 17). Substituting the value of the low-temperature primary rate ($\tau_{rate} \sim 1$ ps) in eq 17 gives

$$6 \text{ ps} \sim \tau_{mix}^{el}/(FC_{in})^{1/2} \sim 2\pi\tau_{rel} \geq \tau_{per} \qquad (18)$$

For such a regime the predictions for τ_{rel} and τ_{per} ($\tau_{rel} \sim 1$ ps and $\tau_{per} \leq 6$ ps) are in agreement with the results of Vos et al. The predictions of golden rule (eq 9) on the other hand, are not as consistent with these results. When we substitute for $\tau_i \sim 1$ ps in eq 9, we get

$$6 \text{ ps} \gg \tau_{mix}^{el}/(FC_{in})^{1/2} \gg 2\pi\tau_{rel} \geq \tau_{per} \qquad (19)$$

That is, for golden rule $\tau_{rel} \ll 1$ ps and $\tau_{per} \ll 6$ ps.

From eqs 18 and 19 we can also make qualitative predictions for the electronic matrix element. If we set $(FC_{in})^{1/2} = 0.2$, a value consistent with $\tau_{per} = 2$ ps,[45] we get $\tau_{mix}^{el} \sim 1$ ps ($V_{el} \sim 30$ cm^{-1}) for the optimal regime, and $\tau_{mix}^{el} \ll 1$ ps ($V_{el} \gg 30$ cm^{-1}) for the golden rule regime. The electronic matrix element needed to achieve a rate of a picosecond is much smaller in the optimal regime than in the golden rule regime. Also, the predicted value of 30 cm^{-1} for the matrix element is a reasonable value, at least in the context of the superexchange mechanism where the bacteriochlorophyll monomer (B) acts a a virtual intermediate for the transfer.[7-9,37]

The question of the validity of the optimal regime in the context of the two-step sequential mechanism[10,11] is more complex. In this case, the bacteriochlorophyll monomer (B) acts as a real intermediate for the electronic transfer. The overall charge separation ($P^*I \rightarrow P^+I^-$) consists of two distinct, incoherent steps; an electron transfer from the excited dimer to the bacteriochlorophyll monomer ($P^*BI \rightarrow P^+B^-I$), and a subsequent transfer from the monomer to the bacteriopheophytin ($P^+B^-I \rightarrow P^+BI^-$). If the rates of the two reactions are similar (it has been suggested that $\tau_{rate} \sim 1$ ps for each one[16]), then both reactions may lie in the optimal regime. For the first reaction, the rate of relaxation in the P^+B^-I vibronic manifold which arises from electron transfer to I ($\tau_{rel} \sim 1$ ps) can compete with the rate of electron transfer from P^*BI to P^+B^-I. Therefore this reaction may be optimal even though the cause of relaxation in P^+B^-I is electronic rather than vibrational. The second reaction may also be optimal if the rate of vibrational relaxation in P^+BI^- is of the order of a picosecond and is thus able to compete with the rate of electron transfer from P^+B^-I to P^+BI^-.

On the other hand, if the rate of the second reaction is much faster than the rate of the first one, as has also been suggested,[37] neither of the two reactions is likely to lie in the optimal regime. In such a situation the first electron transfer from P^*BI to P^+B^-I takes place within a few picoseconds while the second from P^+B^-I to P^+BI^- is faster by at least a factor of 50.[37] Therefore the first transfer cannot lie in the optimal regime since the rate of electronic relaxation in the P^+B^-I manifold is much faster than the transfer rate. The second transfer is too fast to lie in the optimal regime ($\tau_{rate} \leq 0.02$ ps) unless vibrational relaxation in P^+BI^- is also exceptionally high.

The robustness of the rate to changes in vibronic mixing explains certain experiments which indicate that the $P^*I \rightarrow P^+I^-$ rate is largely independent of energy gap, temperature, and degree of initial vibrational excitation in P*I.[46] One set of such experiments involves measurements of the dependence of the rate on the energy gap (ΔE) between P*I and P^+I^-. In particular Lockhart et al.[38,39] have monitored the fluorescence intensity of the excited dimer of *R. sphaeroides* as a function of electric field. Since the fluorescence from P*I competes with the primary charge separation, any change in the primary rate caused by the variation of the energy gap (which is altered by the electric field) affects the fluorescence. They have also used transient absorption spectroscopy[40] to directly measure the $P^*I \rightarrow P^+I^-$ rate. Their experiments suggest that for $\delta\Delta E \sim 300$ cm^{-1} the rate changes by about 20%.[47]

Consistent with this work are the experiments by Fleming et al.[41,42] which measure the temperature dependence of the primary charge separation for both *R. sphaeroides* and *Viridis* using time-resolved absorption spectroscopy. The rate is seen to increase as the temperature is decreased from 200 to 8 K. In *R. sphaeroides* it increases by a factor of only 2 and in *viridis* by a factor of 3.[48]

A nice demonstration of the independence of the rate on the degree of initial excitation in P*I was provided by Middendorf et al.[43] They measured the zero-phonon line width (ZPLW) of P*I for two different RCs. One is the wildtype *R. sphaeroides* and the other a mutant in which the tyrosine adjacent to the BChl monomer of the L branch has been changed to phenylalanine. This substitution greatly reduces the primary rate. The ZPLW is the line width of the ground vibronic state of P*I, $|0\rangle_{P^*I}$. It arises solely from the electronic decay of P*I and from pure dephasing, since the ground vibronic state cannot undergo any vibrational relaxation. Measurement of the ZPLW can therefore give the rate of primary transfer from $|0\rangle_{P^*I}$ if there is not a pure dephasing contribution. Middendorf et al.[43] compare the rates of the mutant and wildtype RCs deduced from the hole widths with those obtained from time-resolved absorption experiments.[49,50] The interesting thing is that for both wildtype and mutant RCs the ZPLW rates at low temperature are very close to those obtained from transient absorption experiments at higher temperature. In particular, the transient absorption rate for the wildtype RCs is (1.9 ps)$^{-1}$ at 80 K, whereas the ZPLW rate is (1.2 ps)$^{-1}$ at 1.5 K. For the mutant RCs the transient absorption rate is (10 ps)$^{-1}$ at 80 K and the ZPLW rate is (8.5 ps)$^{-1}$ at 1.5 K. Since the time-resolved measurements give an average rate arising from several vibrational levels of P*I, this equality indicates that the primary rate from any excited vibrational level of P*I is roughly the same as the rate from the ground vibrational level.[51] The vibrational energy imparted to P*I in these experiments is approximated to be 200–300 cm^{-1}. This robustness of the rate over such an energy range is also observed in the energy gap experiments[38-40] and is consistent with the temperature dependence experiments mentioned above.[41,42] The conclusion is that energy changes of the order of a few hundred cm^{-1} alter the rate by about 20%.[43]

Two explanations have been offered for the independence of rate on initial vibrational excitation.[52] Hayes and Small[53,54] proposed that very fast vibrational relaxation takes place (much faster than a picosecond) from any $|m\rangle_{P^*I}$ to $|0\rangle_{P^*I}$ before the electron transfers. The reaction is therefore independent of initial excitation energy. Middendorf et al.[43] suggested that the primary electron transfer takes place from several vibronic levels of P*I, in parallel, at approximately the same rate (order of a picosecond). If the oscillations observed by Vos et al.[20] are interpreted in terms of vibrational dynamics, then the mechanism of fast vibrational relaxation prior to electronic transfer cannot be valid. On the contrary the oscillations would indicate that the primary electron transfer takes place in parallel at a rate of a picosecond from all the excited levels in P*I. The question which then naturally arises is why the rate changes slowly from vibronic level to vibronic level.

This question can be readily answered by the nonperturbative theory but not by golden rule. We use the results of Middendorf's simulations[43] as an illustration. They use a linear electron–phonon coupling model for $PI + h\nu \rightarrow P^*I$ to self-consistently fit the absorption and holeburning spectra from the two RCs. From this fit they are able to determine with certainty the total Huang–Rhys factor of $PI + h\nu \rightarrow P^*I$ and the inhomogeneous width of the RC sample. They also conclude that at least three modes of low, high, and medium frequencies are necessary to achieve self-consistent fits and predict a range of values for $\hbar\Gamma$, $\hbar\omega$ and for the Huang–Rhys factor S associated with each mode.[55] Let us concentrate on the low-frequency mode which is essential to the validity of the optimal regime in the case of the primary charge separation. For this mode the predictions of the self-consistent

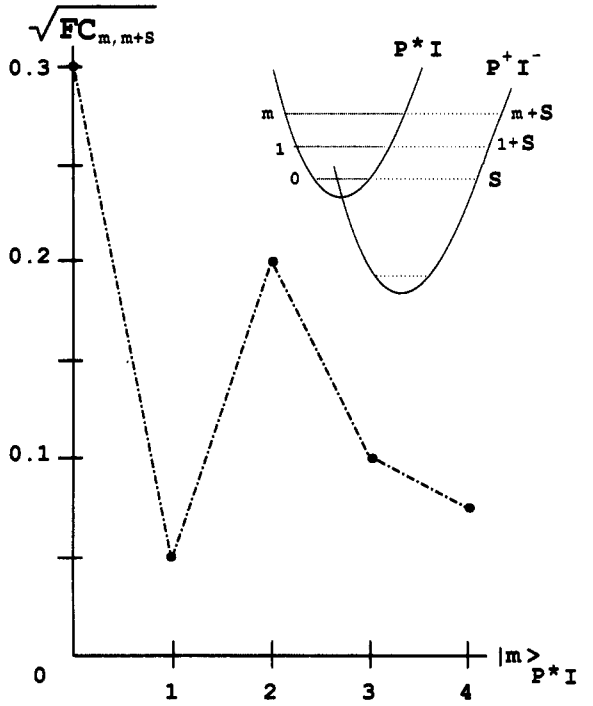

Figure 9. Plot of the square root of the Franck–Condon factor between any initial $|m\rangle_{P^*I}$ vibronic state and any final $|m + S\rangle_{P^+I^-}$ state. The primary transfer is assumed to be activationless with $S = 30$.

fits are as follows: $20\ cm^{-1} \leq \hbar\omega \leq 50\ cm^{-1}$ and $1.7 \leq S \leq 2.6$. We choose the values $\hbar\omega = 40\ cm^{-1}$ and $S = 2$. Our choice means that upon excitation (PI → P*I), roughly $2S = 4$ vibronic levels of a 40-cm^{-1} mode are occupied. We assume that the primary charge separation is activationless with $\lambda \simeq \Delta E \simeq 1200\ cm^{-1}$ and plot in Figure 9 the square root of the Franck–Condon factor between the vibronic states $|m\rangle_{P^*I}$ and $|m + S\rangle_{P^+I^-}$ of the low-frequency mode ($\hbar\omega = 40\ cm^{-1}$, $S = \lambda/\hbar\omega \simeq 30$). We see that in going from $|0\rangle_{P^*I}$ to $|4\rangle_{P^*I}$ (roughly the number of vibronic states excited), $(FC_{m,m+S})^{1/2}$ decreases by $^1/_3$. This means that the sharpest possible decrease of the nonperturbative rate ($\propto (FC)^{1/2}$) is $^1/_3$, whereas the golden rule rate ($\propto$FC) decreases by an order of magnitude.[56]

Another set of experiments which is relevant to this discussion involves measurements of the primary rate of different mutants. Kirmaier et al.[57,58] have measured the primary rate of mutant *R. sphaeroides* and *R. capsulatus* reaction centers. In *sphaeroides* BPh_L has been changed to BChl. The rate decreases by a factor of 2 and the mutation decreases the energy gap by 85 meV (thus decreasing the Franck–Condon factors). This experiment is consistent with the overall picture of 20% variation in the primary rate over changes in energy gap of a few hundred wavenumbers. It is therefore consistent with the optimal regime. In the *R. capsulatus* mutant, the BChl dimer has been changed to a BPh_MBChl heterodimer. The rate decreases by an order of magnitude, but it is not known by how much the vibronic mixing is reduced. The same is true for the mutant used in the Middendorf experiment,[43] where the tyrosine adjacent to $BChl_L$ has been changed to a phenylalanine. All of these mutations decrease the vibronic mixings between initial and final states and thus decrease the rate. However, since we do not know exactly the magnitude of the reduction in the vibronic mixings, we cannot use these experiments to distinguish between optimal and golden rule regimes. If the vibronic mixing could be increased, we would expect the optimal rate to change very little and the golden rule rate to increase considerably by comparison (see Figure 3).

Finally, it should be pointed out that much could be learned from studies of ultrafast electron transfers in model compounds, such as chlorophyll and porphyrin donor–acceptor complexes.[59-61] Such transfers which take place on a time scale of picoseconds or less are likely to lie outside the golden rule regime because they can compete with vibrational relaxation. The behavior of their rates as a function of vibronic mixing and/or vibronic relaxation is a very interesting question.

We have offered a reinterpretation of some experiments without relying on the assumption that the primary rate lies in the nonadiabatic regime. Although recent experiments[20,43] have shed new light on the mechanism of the primary charge separation, they only probe P*I. It is important to simultaneously probe P*I and P^+I^- on a subpicosecond time scale to get the much needed information about the dynamics in P^+I^- on the time scale of the primary charge separation.

Conclusion

We have proposed that the primary charge separation may lie in a regime which is different from that of traditional nonadiabatic (golden rule) theories. The rate in this regime is optimal; that is, it is the maximum possible rate given the values of the other relevant physical parameters of the reacting system.

The motivation behind our proposal has been the high speed of the primary charge separation, which suggests that this reaction may actually compete with vibrational relaxation in the final vibronic manifold of P^+I^-. This is a characteristic of an optimal rate. In contrast, a nonadiabatic rate is much slower than the rate of vibrational relaxation in the final vibronic manifold.

We have shown that the optimal regime is a plausible regime for the primary charge separation. It predicts reasonable values for all the relevant physical parameters of the reaction, and it is consistent with a wealth of experimental information about the primary transfer. In addition, the optimal rate is more robust than the nonadiabatic rate to changes in important reaction parameters such as energy gap and vibronic matrix elements. This property readily explains the apparent independence of the rate to changes in energy gap, temperature, and initial excitation in P*I. The recent experiments by Vos et al.[20] and Middendorf et al.[43] which probe the dynamics of P*I have also been discussed. It was shown how their results provide evidence that supports our proposal.

We want to emphasize that it is necessary to devise experiments which probe the dynamics of P^+I^- on a subpicosecond time scale, as it is formed from P*I. Such experiments will greatly enhance our understanding of the primary charge separation. Right now we can only make inferences about these dynamics from what is observed in P*I.

The suggestion that the primary charge separation may lie in an optimal regime is compelling from a biological point of view. It implies that photosynthetic bacteria make optimal use of the structure of the reaction center for this important ultrafast reaction. Furthermore, the primary rate is resistant to perturbations of the environment.

Acknowledgment. We thank George Feher, Julian Joseph, Thomas Middendorf, William Miller, Mel Okamura, and Andrew Shreve for helpful discussions. J.N.O. is a Beckman Young Investigator. Work in San Diego was supported by the National Science Foundation (Grant No. MCB-9018768), and the Department of Energy's Catalysis/Biocatalysis Program for a research contract administered by JPL. A.J.R.S. acknowledges support from the Brazilian Agency CNPq. J.N.O. is in residence at the Instituto de Física e Química de São Carlos, Universidade de São Paulo, 13560, São Carlos, SP, Brazil during summers.

Appendix I

According to the Green's function formulation of quantum mechanics,[62] the time development operator is the Fourier transform of the Green's function:

$$e^{-i\hat{H}t/\hbar} = \frac{1}{2\pi i}\int_C d\tilde{E}\ e^{-i\tilde{E}t/\hbar}G(\tilde{E}) \tag{20}$$

where the Green's function is given by

$$G(\tilde{E}) = 1/(\tilde{E} - \hat{H}) \tag{21}$$

The Hamiltonian which describes the interaction between one of the initial states $|i\rangle$ in Figure 1 with the $\{|n\rangle\}$ manifold may be

written as $\hat{H} = \hat{H}^0 + \hat{\Delta}$,[24] where

$$\hat{H}^0 = \begin{pmatrix} E_1 & 0 & \cdots & 0 \\ 0 & \tilde{E}_2 & \cdots & 0 \\ \vdots & \vdots & \ddots & \vdots \\ 0 & 0 & \cdots & \tilde{E}_n \end{pmatrix} \tag{22}$$

and

$$\hat{\Delta} = \begin{pmatrix} 0 & \Delta_{12} & \cdots & \Delta_{1n} \\ \Delta_{21} & 0 & \cdots & 0 \\ \vdots & \vdots & \ddots & \vdots \\ \Delta_{n1} & 0 & \cdots & 0 \end{pmatrix} \tag{23}$$

In eqs 22 and 23 $|i\rangle$ has been denoted by $|1\rangle$. Also $\tilde{E}_n = n\hbar\omega - i\hbar\Gamma/2$. In terms of eq 20 the survival amplitude of $|i\rangle$ is given by

$$\langle i|e^{-i\hat{H}t/\hbar}|i\rangle = \frac{1}{2\pi i}\int_C d\tilde{E}\, e^{-i\tilde{E}t/\hbar}\langle i|G(\tilde{E})|i\rangle \tag{24}$$

To obtain an expression for $G(\tilde{E})$, note that

$$G(\tilde{E}) = (\tilde{E} - \hat{H}^0)^{-1}[1 - \hat{\Delta}(\tilde{E} - \hat{H}^0)^{-1}]^{-1} \tag{25}$$

In terms of the zeroth-order Green's function $G^0(\tilde{E}) = [\tilde{E} - \hat{H}^0]^{-1}$ the total Green's function becomes

$$G(\tilde{E}) = G^0(\tilde{E})[1 - \hat{\Delta}G^0(\tilde{E})]^{-1} \tag{26}$$

Expansion of $[1 - \hat{\Delta}G^0(\tilde{E})]^{-1}$ in eq 26 gives

$$G(\tilde{E}) = G^0 + G^0\hat{\Delta}G^0 + G^0\hat{\Delta}G^0\hat{\Delta}G^0 + \ldots \tag{27}$$

so that

$$\langle i|G(\tilde{E})|i\rangle = \langle i|G^0|i\rangle + \langle i|G^0\hat{\Delta}G^0|i\rangle + \langle i|G^0\hat{\Delta}G^0\hat{\Delta}G^0|i\rangle + \ldots \tag{28}$$

$$= \left[\tilde{E} - E_i - \sum_n \frac{\Delta_{in}^2}{\tilde{E} - \tilde{E}_n}\right]^{-1} \tag{29}$$

Substitution of $\tilde{E}_n = n\hbar\omega - i\hbar\Gamma/2$ and of $\Delta_{in} = V_{el}(FC_{in})^{1/2}$ gives eq 4:

$$\langle i|G(\tilde{E})|i\rangle = \frac{1}{\tilde{E} - E_i - V_{el}^2\sum_n (FC_{i,n})\dfrac{(\tilde{E} - n\hbar\omega - i\hbar\Gamma/2)}{(\tilde{E} - n\hbar\omega)^2 + (\hbar\Gamma/2)^2}} \tag{30}$$

To evaluate eq 24, we make use of the residue theorem

$$\langle i|e^{-i\hat{H}t/\hbar}|i\rangle = -\sum_m \mathrm{Res}\,[\langle i|G(\tilde{E})|i\rangle]_{\tilde{E}m} e^{-i\tilde{E}_m t/\hbar} \tag{31}$$

where $\tilde{E}_m$ are the poles of $\langle i|G(\tilde{E})|i\rangle$. The poles are the roots of the secular equation

$$\tilde{E} - E_i = (V_{el}/\hbar\Gamma)^2\sum_n (FC_{i,n})\frac{\tilde{E} - n\hbar\omega - i\hbar\Gamma/2}{((\tilde{E} - n\hbar\omega)/\hbar\Gamma)^2 + 1/2^2} \tag{32}$$

To obtain the golden rule expressions (5) and (6), let $V_{el}(FC_{i,n})^{1/2}$ be much less than $\hbar\Gamma$ in eq 32. Then $\tilde{E} \simeq E_i$. Substituting back into eq 32, we find that

$$\tilde{E} \simeq E_i + (V_{el}/\hbar\Gamma)^2\sum_n FC_{i,n}\frac{E_i - n\hbar\omega - i\hbar\Gamma/2}{((E_i - n\hbar\omega)/\hbar\Gamma)^2 + 1/2^2} \tag{33}$$

so only one pole contributes to the decay amplitude (eq 31) in this limit, and the decay is pure exponential:

$$\langle i|e^{-i\hat{H}t/\hbar}|i\rangle = \frac{1}{2\pi i}(-2\pi i\ \mathrm{Res})e^{-i\tilde{E}t/\hbar} \tag{34}$$

Substitution of eq 34 into expression 2 and performance of the time integrals gives the golden rule rate (eqs 5 and 6).

Appendix II

The Hamiltonian for the two state system in Figure 2 is given by

$$\hat{H} = \begin{pmatrix} 0 & \Delta \\ \Delta & -i\hbar\Gamma/2 \end{pmatrix} \tag{35}$$

If at $t = 0$ the system is in state $|1\rangle$ ($|i\rangle_{P^*1}$) of zero energy, then it can be easily shown that at any time t

$$\langle 1|e^{-i\hat{H}t/\hbar}|1\rangle = \frac{1}{\tilde{E}_+ - \tilde{E}_-}[-\tilde{E}_- e^{-i\tilde{E}_+ t/\hbar} + \tilde{E}_+ e^{-i\tilde{E}_- t/\hbar}] \tag{36}$$

$\tilde{E}_+$ and $\tilde{E}_-$ are the eigenenergies of $\hat{H}$ and are given by

$$\tilde{E}_{+-} = -\frac{i\hbar\Gamma}{4} + -(\Delta^2 + [i\hbar\Gamma/4]^2)^{1/2} \tag{37}$$

The average decay rate of $|1\rangle$ is equal to its inverse lifetime

$$\tau_1^{-1} = \frac{\int_{-\infty}^{\infty} dt\ |\langle 1|e^{-i\hat{H}t/\hbar}|1\rangle|^2}{\int_{-\infty}^{\infty} dt\ t|\langle 1|e^{-i\hat{H}t/\hbar}|1\rangle|^2} \tag{38}$$

Substitution of eq 36 into 38 and performance of the integrals gives

$$\tau_1^{-1} = \frac{1}{\hbar}\frac{F(\tilde{E}_+,\tilde{E}_-)}{H(\tilde{E}_+,\tilde{E}_-)} \tag{39}$$

where

$$F = \frac{|\tilde{E}_+|^2}{2|\mathrm{Im}\ \tilde{E}_-|} + \frac{|\tilde{E}_-|^2}{2|\mathrm{Im}\ \tilde{E}_+|} + 2\ \mathrm{Im}\left[\frac{\tilde{E}^*_-\tilde{E}^*_+}{\tilde{E}^*_+ - \tilde{E}_-}\right] \tag{40}$$

$$H = \frac{|\tilde{E}_+|^2}{(2|\mathrm{Im}\ \tilde{E}_-|)^2} + \frac{|\tilde{E}_-|^2}{(2|\mathrm{Im}\ \tilde{E}_+|)^2} + 2\ \mathrm{Re}\left[\frac{\tilde{E}^*_-\tilde{E}^*_+}{(\tilde{E}^*_+ - \tilde{E}_-)^2}\right] \tag{41}$$

Substitution of the eigenergies in eq 37 into eqs 38–41 and some tedious algebra results in the following expression for the rate

$$\frac{\tau_i^{-1}}{\Gamma} = \frac{4^4x^6 + 3.4^2x^4 - 4x^2}{2.4^4x^6 - 2.4^2x^4 + 4^2x^2 - 1} \tag{42}$$

where $x = \Delta/\hbar\Gamma$.

References and Notes

(1) DeVault, D. *Quantum-mechanical tunneling in biological systems*; Cambridge University Press: Cambridge, 1984.
(2) Hopfield, J. J. *Proc. Natl. Acad. Sci. U.S.A.* **1974**, *71*, 3640.
(3) Jortner, J. *J. Chem. Phys.* **1976**, *64*, 4860.
(4) Feher, G.; Bruker Lecture: Identification and Characterization of the Primary Donor in Bacterial Photosynthesis: A Chronological Account of an EPR/ENDOR Investigation. Submitted to *J. Chem. Soc., Perkin Trans.*
(5) Kirmaier, C.; Holten, D. *Photosynth. Res.* **1987**, *133*, 471.
(6) Feher, G.; Allen, J. P.; Okamura, M. Y.; Rees, D. C. *Nature* **1989**, *339*, 111.
(7) Bixon, M.; Jortner, J.; Michel-Beyerle, M. E.; Ogrodnik, A.; Lersch, W. *Chem. Phys. Lett.* **1987**, *140*, 626.
(8) Creighton, S.; Hwang, J. K.; Warshel, A.; Parson, W. W.; Norris, J. *Biochemistry* **1988**, *27*, 774.
(9) Bixon, M.; Jortner, J.; Michel-Beyerle, M. E.; Ogrodnik, A. *Biochim. Biophys. Acta* **1989**, *977*, 273.
(10) Haberkorn, R.; Michel-Beyerle, M. E.; Marcus, R. A. *Proc. Natl. Acad. Sci. U.S.A.* **1979**, *76*, 4185.
(11) Marcus, R. A. *Chem. Phys. Lett.* **1987**, *133*, 471.
(12) Bixon, M.; Jortner, J.; Michel-Beyerle, M. E. *Biochim. Biophys. Acta* **1991**, *1056*, 301.
(13) Joseph, J.; Bruno, W.; Bialek, W. *J. Phys. Chem.* **1991**, *95*, 6242.
(14) Holzapfel, W.; Finkele, U.; Kaiser, W.; Oesterhelt, D.; Scheer, H.; Stilz, H. U.; Zinth, W. *Chem. Phus. Lett.* **1989**, *160*, 1.
(15) Kirmaier, C.; Holten, D. *Proc. Natl. Acad. Sci. U.S.A.* **1990**, *87*, 3552.
(16) Chan, C. K.; DiMagno, T. J.; Chen, L. X. Q.; Norris, J. R.; Fleming, G. R. *Proc. Natl. Acad. Sci. U.S.A.* **1991**, *88*, 11202.
(17) Ogrodnik, A.; Eberl, U.; Heckmann, R.; Kappl, M.; Feick, R.; Michel-Beyerle, M. E. *J. Phys. Chem.* **1991**, *95*, 2036.

(18) In this paper we do not consider the possibility of a pure dephasing contribution to the widths. We associate widths with relaxation times only, for simplicity of discussion.

(19) Skourtis, S. S. Theoretical Issues in Biomolecular Dynamics. Ph.D. Thesis, University of California Berkeley, Dec, 1991.

(20) Vos, M. H.; Lambry, J. C.; Robles, S. J.; Youvan, D. C.; Breton, J.; Martin, J. L. *Proc. Natl. Acad. Sci. U.S.A.* **1991**, *88*, 8885.

(21) For a Hamiltonian and a more detailed discussion of the calculations to follow see Appendix I.

(22) Bixon, M.; Jortner, J. *J. Chem. Phys.* **1968**, *48*, 715.

(23) Bixon, M.; Jortner, J. *J. Chem. Phys. 50*, 3284.

(24) Freed, K. F. Energy Dependence of Electronic Relaxation Processes in Polyatomic Molecules. In *Radiationless Processes in Molecules and Condensed Phases*; Fong, K., Ed.; Springer-Verlag: Berlin, 1976; pp 23–168.

(25) Equation 4 is the correct Green's function for a discrete spectrum of P^+I^- vibronic states.

(26) Onuchic, J. N.; Goldstein, R. F.; Bialek, W. Biomolecular Dynamics—Quantum or Classical? Results for Photosynthetic Electron Transfer. In *Perspectives in Photosynthesis, Proceedings of the 22nd Jerusalem Symposium on Quantum Chemistry and Biochemistry*; Jortner, J., Pullman, B., Eds.; D. Reidel Publishing Co.: Dordecht, Holland, 1989; pp 211–226.

(27) Expression 6 is approximate. We do not expect all line shapes to be Lorentzians since not all levels will experience the same, ohmic damping. However the sum should not be thought of as an infinite sum. It should only contain contributions from the few $|n\rangle_{P^+I^-}$ which are closest in energy to $|i\rangle_{P^*I}$ and experience roughly the same damping.

(28) Equation 8 holds for a discrete final vibronic spectrum (see ref 25). In deriving this equation, we have not specified the amount by which V_{el} is smaller than $\hbar\Gamma$. It turns out that the regime defined by this equation involves values of $(FC)^{1/2}V_{el} \leq 0.1\hbar\Gamma$ and $\tau_i^{-1}/\Gamma \leq 0.05$. For this range of values the golden rule expression 5 is exact. However there exists another regime with higher $(FC)^{1/2}V_{el}$ for which expression 5 is not exact but gives values close to the actual rate. In this region eq 8 breaks down, and the relevant parameters do not exhibit order of magnitude differences. This regime might be relevant to the primary charge separation. For the purposes of the discussion given here, we will always refer to the "exact" golden rule regime given by eqs 8 and 9.

(29) Onuchic, J. N.; Wolynes, P. G. *J. Phys. Chem.* **1988**, *92*, 6495.

(30) Onuchic, J. N. *J. Phys. Chem.* **1987**, *85*, 3925.

(31) Onuchic, J. N.; Beratan, D. N. *J. Phys. Chem.* **1986**, *90*, 3707.

(32) Alfano, R. R.; Shapiro, S. L. *Phys. Rev. Lett.* **1971**, *26*, 1247.

(33) Laubereau, A.; Wochner, G.; Kaiser, W. *Opt. Commun. 14*, 75.

(34) McCammon, J. A.; Harvey, S. C. *Dynamics of proteins and nucleic acids*; Cambridge University Press: Cambridge, 1987.

(35) Of course we could achieve any rate within the golden rule regime by allowing for a large enough density of final states ($\hbar\Gamma > \hbar\omega$). We would then have the problem of justifying the anomalous density of states.

(36) See discussion of the experiments by Vos et al.[20] and by Middendorf et al.[43] in the relevant section.

(37) Bixon, M.; Jortner, J.; Plato, M.; Michel-Beyerle, M. E. Mechanism of the Primary Charge Separation in Bacterial Photosynthetic Reaction Centers. In *Proceedings of a NATO Advanced Research Workshop on the Structure of the Photosynthetic Reaction Center*, Breton, J., Vermeglio, A., Eds.; Plenum Press: New York, 1987, pp 399–420.

(38) Lockhart, D. J.; Goldstein, R. F.; Boxer, S. G. *J. Chem. Phys.* **1988**, *89*, 1408.

(39) Lockhart, D. J.; Boxer, S. G. *Chem. Phys. Lett.* **1988**, *144*, 243.

(40) Lockhart, D. J.; Kirmaier, C.; Holten, D.; Boxer, S. G. *J. Phys. Chem.* **1990**, *94*, 6987.

(41) Fleming, G. R.; Martin, J. L.; Breton, J. *Nature* **1988**, *333*, 190.

(42) Martin, L. J.; Breton, J.; Lambry, C.; Fleming, G. R. The primary electron transfer in photosynthetic bacteria: long range electron transfer in the femtosecond domain at low temperatures. In Breton; J., Vermeglio, A., Eds.; *The Photosynthetic Bacterial Reaction Center. Structure and Dynamics*; Plenum: New York, 1988; pp 113–118.

(43) Middendorf, T. R.; Mazzola, L. T.; Gaul, D. F.; Schenck, C. C.; Boxer, S. G. *J. Phys. Chem.* **1991**, *95*, 10142.

(44) The inequality $\hbar\Gamma \leq \hbar\omega$ means that the P^+I^- spectrum must be discrete. If $\hbar\Gamma$ is greater than $\hbar\omega$, the P^+I^- spectrum becomes a dense continuum and we enter a golden rule regime which will not be discussed here (see ref 35).

(45) This is approximately the correct value for the lowest lying vibronic states of P*I if we assume that the primary charge separation is activationless with reorganization energy of 1200 cm^{-1} and that it couples to a 16 cm^{-1} (2 ps) mode as suggested by the Vos experiment.

(46) These experiments were correlated in the recent paper by Middendorf et al.[43] Part of our discussion is based on this paper.

(47) For possible challenges to such an inference see: Ogrodnik, A.; Eberl, U.; Haberle, T.; Keupp, W.; Langenbacher, T.; Siegl, J.; Volk, M.; Michel-Beyerle, M. E. *Biophys. J.* **1992**, *61*, A152, 873. Franzen, S.; Lao, K. Q.; Stanley, B.; Boxer, S. G. *Biophys. J.* **1992**, *61*, A153, 874.

(48) This robustness to temperature changes has led to the proposal that the primary charge separation is activationless. It should be pointed out however that temperature independence can also arise from activated geometries if the transfer is not significantly coupled to low-frequency modes (see Friesner, R. A.; Won, Y. *Biochim. Biophys. Acta* **1989**, *977*, 99).

(49) Kirmaier, C.; Holten, D. *Photosynth. Res.* **1987**, *13*, 225.

(50) Nagarajan, V.; Parson, W. W.; Gaul, D.; Schenck, C. *Proc. Natl. Acad. Sci. U.S.A.* **1990**, *87*, 7888.

(51) It also indicates that there is no contribution to the ZPLW from pure dephasing.

(52) Here we exclude the possibility of coupling to only high frequency modes in view of the results of Vos et al.

(53) Tang, D.; Johnson, S. G.; Jankowiak, R.; Hayes, J. M.; Small, G. J.; Tiede, D. M. In Jortner, J., Pullman, P., Eds.; *Perspectives in Photosynthesis*, Kluwer Academic Publishers: 1990; pp 99–120.

(54) Johnson, S. G.; Tang, D.; Jankowiak, R.; Hayes, J. M.; Small, G. J.; Tiede, D. M. *J. Phys. Chem.* **1990**, *94*, 5849.

(55) The values for S, $\hbar\Gamma$, and $\hbar\omega$ for each mode are not predicted with certainty like those of the inhomogeneous distribution width and the total Huang–Rhys factor. A larger number of modes each with smaller S or with smaller $\hbar\omega$'s is as good as three modes as long as the total S remains constant. Also the individual homogeneous widths $\hbar\Gamma$ can afford to decrease if the total number of modes increases. The predictions are consistent with recent resonance Raman data on the special pair discussed in: Shreve, A. P.; Cherepy, N. J.; Franzen, S.; Boxer, S. G.; Mathies, R. A. *Proc. Natl. Acad. Sci. U.S.A.* **1991**, *88*, 11207.

(56) We would like to emphasize that the issue of the rate of thermalization in P*I is by no means resolved. However, the robustness of the primary rate with respect to changes in temperature is a well-established fact, and this robustness is a natural consequence of the optimal regime.

(57) Kirmaier, C.; Holten, D.; Bylina, E. J.; Youvan, D. C. *Proc. Natl. Acad. Sci. U.S.A.* **1988**, *85*, 7562.

(58) Kirmaier, C.; Gaul, D.; DeBey, R.; Holten, D.; Schenck, G. C. *Science* **1991**, *251*, 922.

(59) Vergeldt, F. J.; Koehorst, R. B. M.; Schaafsma, T. J.; Lambry, J. C.; Martin, J. L.; Johnson, D. G.; Wasielewski, M. R. *Chem. Phys. Lett.* **1991**, *182*, 107.

(60) Wasielewski, M. R.; Johnson, D. G.; Niemczyk, M. P.; Gaines III, G. L.; O'Neil, M. P.; Svec, W. A. Solvent-Dependent Photophysics of Fixed-Distance Chlorophyll-Porphyrin Molecules: The Possible Role of Low-Lying Charge-Transfer States. In *Electron Transfer in Inorganic, Organic, and Biological Systems*; Advances in Chemistry Series, No. 228; Bolton, J. R., Mataga, N., McLendon, G., Eds.; American Chemical Society: Washington, DC, 1991; pp 133–148.

(61) Tetrahedron-Symposia-in-Print, number 39, Covalently Linked Donor-Acceptor Species for Mimicry of Photosynthetic Electron and Energy Transfer, Gust, D.; Moore, T. A., editors; *Tetrahedron* **1989**, 45.

(62) Messiah, A. *Quantum Mechanics*; Wiley: New York, Vol. 2.